A Dendronized Polymer Is a Single-Molecule Glass†

Jayajit Das,[‡,||] Masaru Yoshida,[§] Zachary M. Fresco,[§] Tae-Lim Choi,[§] J. M. J. Fréchet,[‡,§,||] and Arup K. Chakraborty*[,‡,§,||,⊥]

Departments of Chemical Engineering and Chemistry, University of California—Berkeley, Berkeley, California 94720, and Materials Science Division and Physical Biosciences Division, Lawrence Berkeley National Laboratory, Berkeley, California 94720

Received: March 4, 2005

The molecular architecture of dendronized polymers can be tuned to obtain nanoscale objects with desired properties. In this paper, we bring together experiments and computer simulations to study the thermodynamic and dynamic properties of a single dendronized polymer chain. We find that, upon changing certain architectural features, dynamic correlations characterizing backbone conformational fluctuations of a dendronized polymer exhibit dynamics akin to glass-forming bulk liquids. Thus, a dendronized polymer chain is a novel macromolecule that is a single-molecule glass. Over a range of conditions that lead to glassy dynamics, there does not appear to be any thermodynamic singularities. We discuss how a dendronized polymer is a molecular system that can directly test different models of glassy dynamics. We also show that defect densities characteristic of typical synthesis conditions do not alter the material properties of dendronized polymers.

Introduction

Dendronized polymers are novel macromolecules whose nanoscale size, rigidity, and functionality can be controlled with precision by tuning molecular architecture.[1−3] A typical dendronized polymer is composed of a backbone such as polystyrene or polyacrylate with pendant reactive anchor groups, from each of which emerges a dendron (Figure 1a). The dendron units have a regular branching pattern with each repeat unit contributing a branch point, and synthetic procedures have been developed to control the number of generations of dendritic growth precisely. The size of each dendron varies from about 0.3−0.5 nm to well over 1.0 nm depending upon the specific nature of the repeat unit and the number of generations.

By manipulating the size and the number of generations characterizing a dendron, the flexibility of a dendronized polymer can vary from a lithe Gaussian chain to rigid nanoscale objects (Figure 1b). Here, we report findings that demonstrate that a single dendronized polymer chain exhibits dynamical arrest as the number of generations composing the pendant dendron increases. A dendronized polymer is thus a single-molecule glass, a kind of molecular matter first imagined by deGennes.[4] Specifically, we find that fluctuations of the backbone conformations exhibit dynamic correlations that are characterized by stretched exponential kinetics beyond a threshold number of dendron generations. However, the thermodynamic features (or static correlations) do not appear to exhibit singularities over the same range of conditions. This behavior of a single molecule is reminiscent of dynamical arrest observed in theoretical and computational studies of facilitated kinetic spin models.[5−9] Indeed, we suggest that the molecular architecture of a dendronized polymer results in backbone conformational fluctuations that could be described by dynamic facilitation rules. Dendronized polymers with even higher number of generations appear to exhibit a divergent relaxation time for the dynamics of backbone fluctuations. Although previous observations[10] of the lack of flexibility of high-generation dendronized polymers have led to speculation that they may share features with glasses, our studies show that dendronized polymers provide the first example of a molecular experimental system that can enable direct tests of models for glassy dynamics. This is because, over a range of conditions, as in facilitated spin models, the interesting behavior we describe appears to originate from purely dynamic constraints rather than underlying thermodynamic features. Furthermore, for high-generation (≥ 4) dendronized polymers, the density of dendron segments near the periphery of the chain can approach a close-packing limit. Similar random close-packing can give rise to glassy behavior in a system of hard spheres.[11−14] Models that describe the physics of such a jamming limit can also thus be studied carefully by applying single-molecule experimental methods to dendronized polymers. Experiments testing our predictions should also help to establish the existence of a new class of single-molecule behavior—a single molecule that exhibits glassy dynamics. We emphasize that our discovery of a molecule that exhibits apparently glassy single-molecule dynamics as its molecular architecture is tuned does not have a direct bearing on controversies regarding the origin of dynamic arrest in bulk glass-forming liquids upon cooling.[5,9,15−19]

In the following text, we first provide a brief description of the computational and experimental methods used in our work. This is followed by a brief discussion of our results for the static correlations that describe the thermodynamics of dendronized polymers. Then, we describe our results showing that conformational fluctuations of a single dendronized polymer undergo dynamical arrest as the number of generations increases. We also study the effects of defects that may occur during the

† Part of the special issue "David Chandler Festschrift".

* To whom correspondence may be addressed. E-mail: arup@uclink.berkeley.edu.

‡ Department of Chemical Engineering, University of California—Berkeley.

§ Department of Chemistry, University of California—Berkeley.

|| Materials Science Division, Lawrence Berkeley National Laboratory.

⊥ Physical Biosciences Division, Lawrence Berkeley National Laboratory.

10.1021/jp058081e CCC: $30.25
Published on Web 03/26/2005

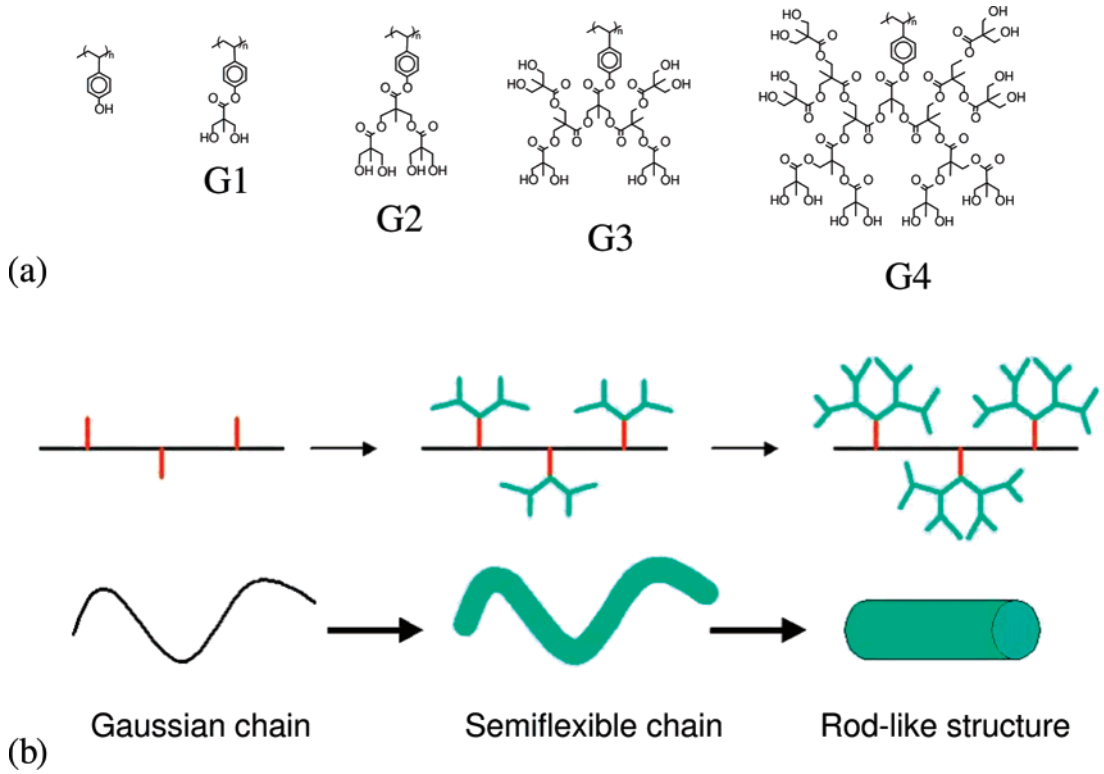

Figure 1. (a) Chemical structure of dendron units from the first to the fourth generation. (b) Schematic pictures showing flexibility increases from that of a Gaussian chain to rodlike structures as the number of generations increases.

TABLE 1: Molecular Weight and Radius of Gyration of Dendronized Polymers Determined by Multiangle Laser Light Scattering (MALLS) Measurements

compound (N_g)	theor. M_w[a] ($DP_w = 1280$)	obsd M_w	PDI[b]	DP_w[c]	$R_{g,z}$ (nm)[d]
PHS-150K-OH (0)	153 000	153 000	1.05	1280	15.1 ± 0.45
G1-OH_2 (1)	302 000	286 000	1.06	1210	18.3 ± 0.49
G2-OH_4 (2)	598 000	567 000	1.08	1210	23.6 ± 0.42
G3-OH_8 (3)	1 190 000	1 120 000	1.06	1200	27.6 ± 0.33
G4-OH_{16} (4)	2 380 000	2 360 000	1.06	1260	32.0 ± 0.42

[a] Based on the SEC-MALLS data of PHS. [b] Polydispersity indices (M_w/M_n). [c] Weight-averaged degree of polymerization. [d] Errors were calculated from a combination of baseline noise assessment and the quality of the fit in the Debye plot.

construction of the dendrons. Two results are emphasized in this regard. First, the fraction of defects that is typical of a well-planned divergent synthesis does not have any practical consequence on the rigidity of a dendronized polymer. When the fraction of defects (defined as the fraction of absent groups in a generation of a dendron) decreases beyond a threshold value, there is a sharp decrease in flexibility due to a percolation transition on a non-Euclidean manifold. Second, tuning the fraction of defects (for a fixed number of generations) also leads to glassy dynamics.

Experimental and Computational Methods

Synthesis of Dendronized Polymers and Measurement of the Radius of Gyration. Poly(*p*-hydroxystyrene) (**1**) (M_w = 153 kDa, PDI = 1.05 by MALLS) was a gift of the Nippon Soda Company (Chiba, Japan). Divergent dendronization was carried out using benzylidene- and isopropylidene-2,2-bis-(oxymethyl)propionic anhydrides according to literature procedures.[20] Size-exclusion chromatography (SEC) combined with multiangle laser light scattering (MALLS) measurements was performed in DMF containing 0.2 wt % LiBr as the mobile phase using a system composed of a Waters 510 pump, a Rheodyne injector with 50 μL sample loop, two PLgel mixed-bed C (7.8 × 300 mm^2) columns thermostated at 70 °C, and a Dawn EOS MALLS and Optilab DSP differential refractometer thermostated at 35 °C. The flow rate was 0.8 mL/min. The light source was a GaAs laser with 690 nm wavelength and 30 mW output power as measured at 685 nm. Scattering signals were collected at 17 different angles from 20 to 153°. The data were analyzed using ASTRA for Windows software (version 4.90.07, Wyatt Technology), and Zimm plots (K^*c/R) were used for the detector fitting method. The absolute molecular weights of the dendronized polymers were determined using the MALLS data and two additional parameters: (i) the known RI detector calibration constant and (ii) an assumption of 100% mass recovery of the injected polymer sample. Typically, for both SEC and SEC-MALLS measurements, 1−2 mg/mL of polymer solution was prefiltered through 0.2 μm pore size PTFE filters (Whatman) before injection.

Computer Simulation Algorithm. We perform an off-lattice Monte Carlo (MC) simulation of a single dendronized polymer.[21] The backbone, composed of N monomers and arc length $L = Nl_0$, is represented by a bead−spring model.[22] Two neighboring monomers are connected by a simple harmonic potential $U(l) = k(l - l_0)^2$ for $l_{min} < l < l_{max}$ and $U(l) = \infty$ otherwise. The monomers interact via a hardcore interaction potential where the radius of each monomer is $0.4r_C$ and l_0 is set to $0.7r_C$; l_{max} and l_{min} are taken to be r_C and $0.4r_C$, respectively. The characteristic length scales are set by r_C, which is taken to be unity. We set $k/k_BT = 1$. This set of parameters ensures that monomers do not cross each other during the simulation. Each monomer is attached to a dendron unit by a connector of length l_{conec}. The connector is modeled by two spherical subunits that are immobile and change positions only through center-of-mass movements. The dendron units are represented by a set of spherical subunits, each of radius r_S connected according to the

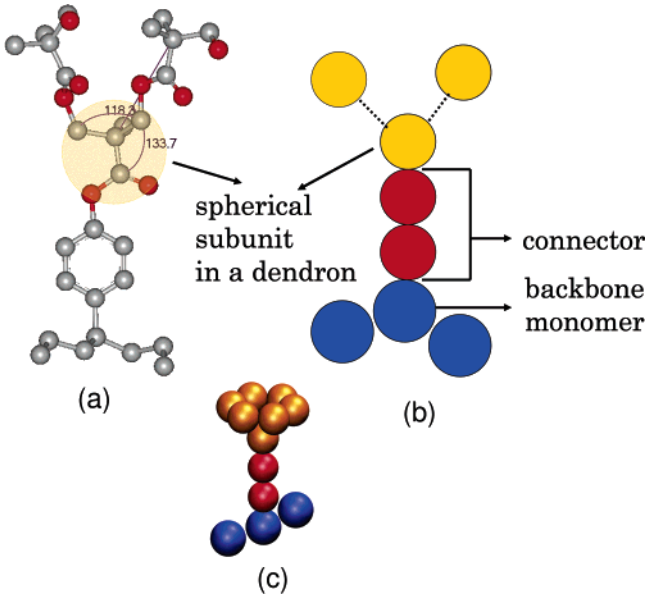

Figure 2. (a) Coarse-graining scheme used, which is shown for a second-generation dendron unit. Each dendron unit, marked by the shaded area, is represented by a sphere of diameter 0.216 nm. The connector is modeled by two spheres (shown in red in b), each of diameter 0.216 nm. (b) Coarse-grained unit. The dendron subunits interact via a harmonic potential $E = E_{stretch} + E_{bend}$ where the bond stretching is represented by $E_{strech} = k_{stretch}(R - R_0)^2$ for $R < R_{max}$; R is the distance between the centers of neighboring subunits, $R_0 = 0.216$ nm, and $R_{max} = 0.7$ nm (van der Waals radius of the unit). $E_{stretch}$ is irrelevant outside the domain. We take $k_{stretch}/k_BT = 2555$ nm^{-2}. The bending energy is represented by $E_{bend} = k_{rot}(\cos(\theta) - \cos(\theta_0))^2$, where $\theta_0 = 133.7°$. Because k_{rot} is not known, we vary k_{rot} from the extremely flexible ($k_{rot}/k_BT = 1$) to the rigid ($k_{rot}/k_BT = 1200$) in the simulations. The subunits in the connectors are immobile and change positions only through center-of-mass movements. (c) Torsion degrees of freedom are accounted for by including spherical subunits in locations that can be accessed by torsional motion.

hierarchical structure of a dendron unit (Figure 2a). The spherical subunits interact via harmonic potentials describing bond stretching and angle bending. The torsional degrees of freedom are not explicitly accounted for because they are almost 20 times faster than the vibrational and bending modes. Spherical subunits are introduced to account for the steric interactions at locations that are accessible because of torsional degrees of freedom. The force fields describing interactions between the dendron subunits are taken from DREIDING.[23] We have taken $r_S = 0.3375r_C$ and $l_{conec} = 4r_S$. The interactions between the spherical subunits in different cones and between the monomers are described by hard-core repulsion. The parameters used in the model are set by the molecular system that we synthesize (vide supra). Figure 2 describes the correspondence between the coarse-grained model and the chemical constitution of the molecules used in our experiments.

In a MC trial, a spherical subunit in a dendron unit is chosen for an attempted move according to the ratio of the diffusive time scales characterizing a spherical subunit and a whole dendron unit. If a spherical subunit is not chosen, either a backbone monomer or the dendron unit is chosen to move with equal probability. Each trial is accepted or rejected on the basis of a Metropolis sampling scheme.[24] In a trial, a backbone monomer is displaced in a random direction within a cube of size l_{max} with the old monomer position defining the center of the cube. Entire dendrons move by rigid rotations. The rigid rotation of each dendron is described by three Euler angles ϕ, ψ, and θ . A random increment in ϕ, ψ, and $\cos(\theta)$ is attempted, and detailed balance is enforced in the simulations. We simulate molecules where $N = 33$, 41, and 51, and generation number N_g is varied from 1 to 4. All of the data are collected after 10^6 MCS.

Molecular crowding leads to defects in synthesis[20,25] for higher generations (such as the fourth generation). A fractional defect density equal to p is introduced in the following way in the simulations. Spherical subunits are chosen in a particular generation with a probability p drawn from a uniform random distribution, and all of the subunits originating from that particular subunit are removed from the dendron unit.

Quantities Calculated. We evaluate quantities such as the radius of gyration (R_g) and bond correlation function $C(s)$ to study the change in flexibility of the backbone and the dynamic correlations that describe conformational fluctuations. The radius of gyration is defined as

$$R_g^2 = \left\langle \frac{1}{N}\sum_{i=1}^{N}(R_i - R_{cm})^2 \right\rangle \quad (1)$$

where R_i the position of the ith bead, $R_{cm} = {}^1/_N \sum_{i=1}^{N} R_i$ is the center of mass, and $\langle\cdots\rangle$ denotes an average over equilibrium configurations. The bond correlation function $C(s)$ is given by $C(s) = \langle {}^1/_N \sum_{i=1}^{N} u_i \cdot u_{i+s}\rangle$ where $u_i = (R_{i+1} - R_i)/|R_{i+1} - R_i|$ is the local tangent vector.

The flexibility of the chain can be quantified by the persistence length (L_P) of the backbone, which can be estimated both from the radius of gyration (R_g) and $C(s)$ using the expression for a semiflexible chain from the Kratky Porod (KP) model.[26] These quantities are given by

$$R_g^2 = \frac{LL_p}{3} - L_p^2 + \frac{2L_p^3}{L} - \frac{2L_p^4[1 - \exp(-L/L_p)]}{L^2} \quad (2)$$

and

$$C(s) = \exp\left(-\frac{s}{L_p}\right) \quad (3)$$

To investigate chain dynamics, we calculate the time-dependent correlation function

$$C(s, t, t') = \left\langle \frac{1}{N}\sum_{i=1}^{N} u_i(t) \cdot u_{i+s}(t') \right\rangle \quad (4)$$

Results

Conformational Statistics. Figure 3a shows how R_g varies with the number of generations for $N = 33$. We show results for flexible ($k_{rot}/k_BT = 1$) and rigid ($k_{rot}/k_BT = 1200$) dendrons. For $N_g = 1$ and $N_g = 2$, there are no differences as dendron rigidity is changed. For $N_g < 3$, the decrease in the available space due to increased dendron flexibility is a small effect because molecular crowding is not important. The effect of dendron flexibility is prominent only for $N_g > 3$, where flexible dendron units render the backbone more rigid. This is because a more flexible dendron is more spherical compared to a rigid dendron unit, which has a "broccoli"-like shape with the connector acting as the stem. The drooping sphere-like shape of flexible dendrons reduces the available space for backbone monomer fluctuations, thus making the backbone more rigid.

We carried out experiments with chains characterized by $N = 1280$ monomers.[25] Simulations of such long chains are very computationally intensive; therefore, we extrapolated results from the computer simulations for direct comparison with experiments. For $N_g = 1$ and $N_g = 2$, our simulation results

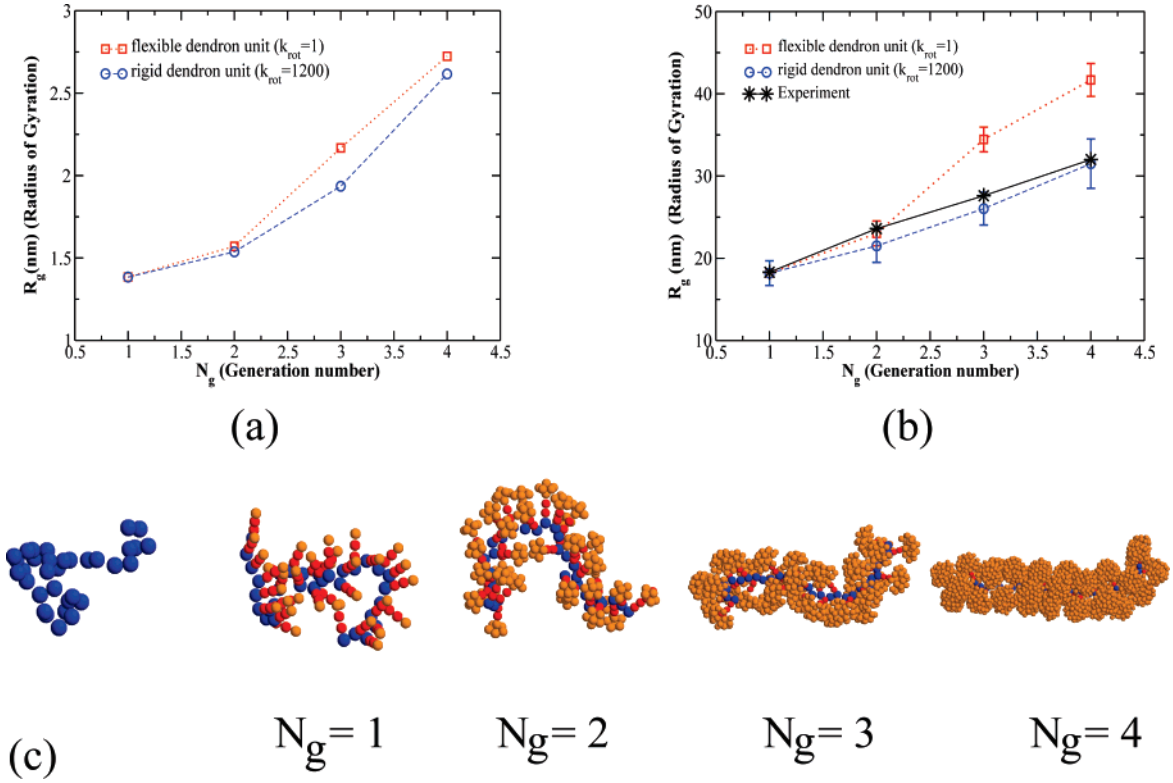

Figure 3. (a) Radius of gyration (R_g) for a chain with 33 backbone monomers increases continuously as the number of generations (N_g) is increased from 1 to 4. The dendron flexibility has a minimal effect. (b) Variation of R_g with N_g for the long chains studied in experiments. The simulation results were obtained using the extrapolation methods described in the text. Error bars are shown if they are larger than the symbol size, and the calculated points are joined by lines to guide the eye. The agreement is excellent for all generation numbers for simulations carried out using rigid dendrons. (c) Configurations for various dendron generations shown for a backbone of 33 monomers. Note the gradual change from flexible to rodlike structures as N_g increases.

exhibit a power law scaling, $R_g = AN^{\alpha}$. We extract A and α to obtain extrapolated values for R_g. For $N_g = 4$, we can fit our results with the Kratky Porod model.[26] We extract the persistence length, L_p, and use that to evaluate R_g for long chains. But for $N_g = 3$, neither a scaling law nor the Kratky Porod model fit our simulation results. This is because $N_g = 3$ corresponds to a crossover regime between flexible and semiflexible chain characteristics. Therefore, we use the scaling behavior of R_g with the number of branch points in a dendron unit to extrapolate results for $N_g = 3$. To carry out this scaling analysis, we followed the methods described in refs 27 and 28. Figure 3b shows comparisons between the experiments and the extrapolated simulation data. The agreement is excellent for all generation numbers for simulations carried out using rigid dendrons. Regardless of the details of the comparisons between experiments and simulation results, the key finding that emerges from Figure 3 is that the variation of R_g with N_g is smooth and monotonic. Under the range of conditions that we consider, our computer simulation results and experimental measurements seems to exhibit no thermodynamic singularities. (For further details on the possibility of thermodynamic anomalies, see ref 29 and discussions that follow.) As we shall see, this is in sharp contrast to the dynamics characterizing conformational fluctuations.

During synthesis, defects start arising from the fourth generation.[20,25] Figure 4a shows how R_g varies with the defect density (p). Dendron flexibility does not have any appreciable effect on the variation of R_g with p. The effect of defects on the backbone rigidity is not prominent until it exceeds approximately 50%. This asserts that the approximately 10% fraction of defects introduced by following typical synthetic procedures is irrelevant for material properties. The shape of the curve in Figure 4a hints at a percolation transition.[30] To investigate if there is an underlying percolation transition, we calculated the connected cluster of dendron subunits. Two sites are taken to be connected if the distance between their centers is less than $2r_S + \epsilon$, where r_S is the radius of a spherical subunit and ϵ is a small number, $\sim 0.4r_S$. The qualitative results are insensitive to small variations in ϵ. We calculated the average values (S_L) of system-spanning clusters. A cluster is considered to span the whole system if members of the cluster belong to the first and last dendron units of the backbone. In an ideal percolation transition, $S_L = 1$ and $S_L = 0$ above and below the percolation transition, respectively. We study cases where the defects start occurring in the fourth generation.[25] We find (Figure 4b) $S_L \approx 1$ for $p < 0.5$ and $S_L < O(10^{-2})$ for $p > 0.5$ for rigid dendron units. The transition occurs at a larger value of p when the dendron units are flexible. This suggests a continuum percolation[30−32] in the dendron subunits. However, we need to consider larger system sizes and follow a rigorous scaling analysis to quantify the nature of the percolation transition. We point out that our finding (Figure 4b) relates to issues pertinent to percolation transitions in objects embedded in a non-Euclidean manifold. In our case, the curved shape of the polymer backbone provides such a manifold (Figure 4c), and a manifestation of this is that the value of p at which the transition occurs is different compared to cases where the manifold is not curved.

Dynamics. Although the static correlations at equilibrium for a dendronized polymer exhibit smooth crossovers from characteristics of flexible to semiflexible chains as the number of generations increase, our simulations show that the dynamic correlations show signatures of glassy dynamics beyond a threshold value of N_g. Figure 5a shows snapshots of configura-

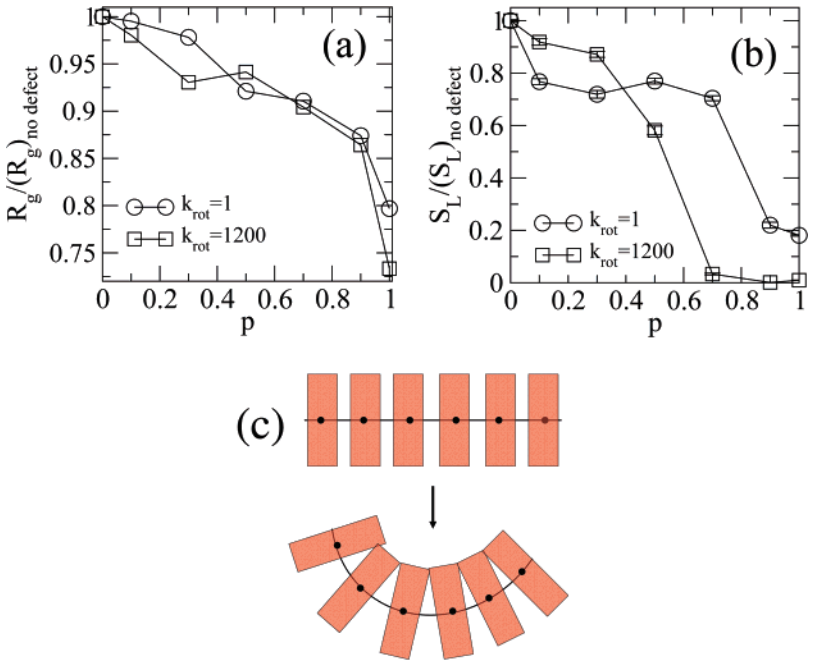

Figure 4. (a) Effect of defects on the radius of gyration. The defects are present only in the fourth generation with a fraction p. The variation of R_g (normalized by R_g for a chain with no dendrons) with p shows that the decrease in the value of R_g is appreciable only beyond $p > 0.5$. Also, note that the flexibility of the dendron units has no appreciable effect. (b) Plot of the average density of the system spanning clusters (S_L) with p. The results suggest a percolation transition. (c) Cartoon in one dimension demonstrating how the curvature in the embedding manifold can result in connected clusters for values of p that are larger than that for a flat manifold.

tions obtained from our MC simulations for dendronized polymers with different values of N_g (movies are available in a web supplement). These snapshots indicate that backbone conformations relax much more slowly as N_g increases. The decay of dynamic correlations can be monitored by the following quantity:

$$A(t', t) = \frac{1}{N-1}\sum_{i=1}^{N-1}\sigma(i, t')\,\sigma(i, t) \qquad (5)$$

where $\sigma(i, t)$ is an Ising-like order parameter defined as $\sigma(i, t) = sgn[u(i, t)\cdot u(i + 1, t)]$. The reason that we consider this quantity rather than $C(i, i'; t, t')$ will be made clear below. Figure 5b shows how $A(t, t')$ decays with time. As is clear, when N_g is small, we find that backbone conformational fluctuations exhibit a standard Debye or exponential decay. However, for $N_g \geq 3$, the autocorrelation function decays much more slowly and can be fit by a stretched exponential function. The onset of the stretched exponential decay of correlations is often used as a signature of "glassy" behavior in bulk liquids.[15,18,33,34] Figure 5c shows the variation of the relaxation time (extracted from results in Figure 5b) with the number of generations that comprise the dendron units. There is an apparent divergence of relaxation times, another feature characteristic of dynamic arrest and supercooled liquids. It is important to note, however, that we are not changing temperature but rather tuning an architectural parameter of a macromolecule to access behavior that resembles supercooling in bulk liquids. The results shown in Figure 5 lead us to the conclusion that a dendronized polymer is a single-molecule glass with an onset of glassy dynamics when the number of generations characterizing the pendant dendrons exceeds a threshold value.

The transition between the stretched exponential decay of correlations and the Debye relaxation of backbone conformational fluctuations can also be observed by introducing defects in the dendron units. For example, consider a dendronized polymer with $N_g = 3$. When there are no defects, the correlation function decay is characterized by a stretched exponential. We then introduce defects with a probability p starting from the second generation. We find an exponential decay of correlations when the defect density is sufficiently high.

Figure 6a shows that β approaches unity as the defect density becomes large and decreases to small values with a diverging relaxation time scale as the defect density becomes small. Figure 6b shows that β also decreases with N_g for dendronized polymers with a small defect density.

The physical origin of the behavior described above is that the dynamics of backbone conformational fluctuations is influenced by the dynamics of the dendrons. For a backbone segment to move, the dendrons must also move. When the number of generations constituting each dendron is large, steric hindrance between dendron subunits and the fact that each dendron is connected to backbone segments constrain the translational and rotational motility of the dendrons. This, in turn, restricts the mobility of backbone segments. Thus, a series of constraints determines the dynamics of a single dendronized polymer chain when each dendron is composed of many generations. These constraints on the dynamics are not manifested when N_g is small because steric constraints between subunits of adjacent dendrons are not important.

The constraints determining the dynamics of a dendronized polymer chain are reminiscent of constrained or facilitated dynamical models of glass-forming liquids.[5,8,9,21,35] The degrees of freedom in simple versions of these models are Ising spins that can flip between two states. A given Ising spin can flip only if a set of conditions (postulated phenomenologically) are obeyed by its neighboring spins. The constraints applied by the dendrons on the backbone, and vice versa, share similar qualitative features. However, these constraints are more complicated. The steric interactions between neighboring dendrons that are also constrained by being attached to backbone segments result in effective constraints (facilitation rules) that

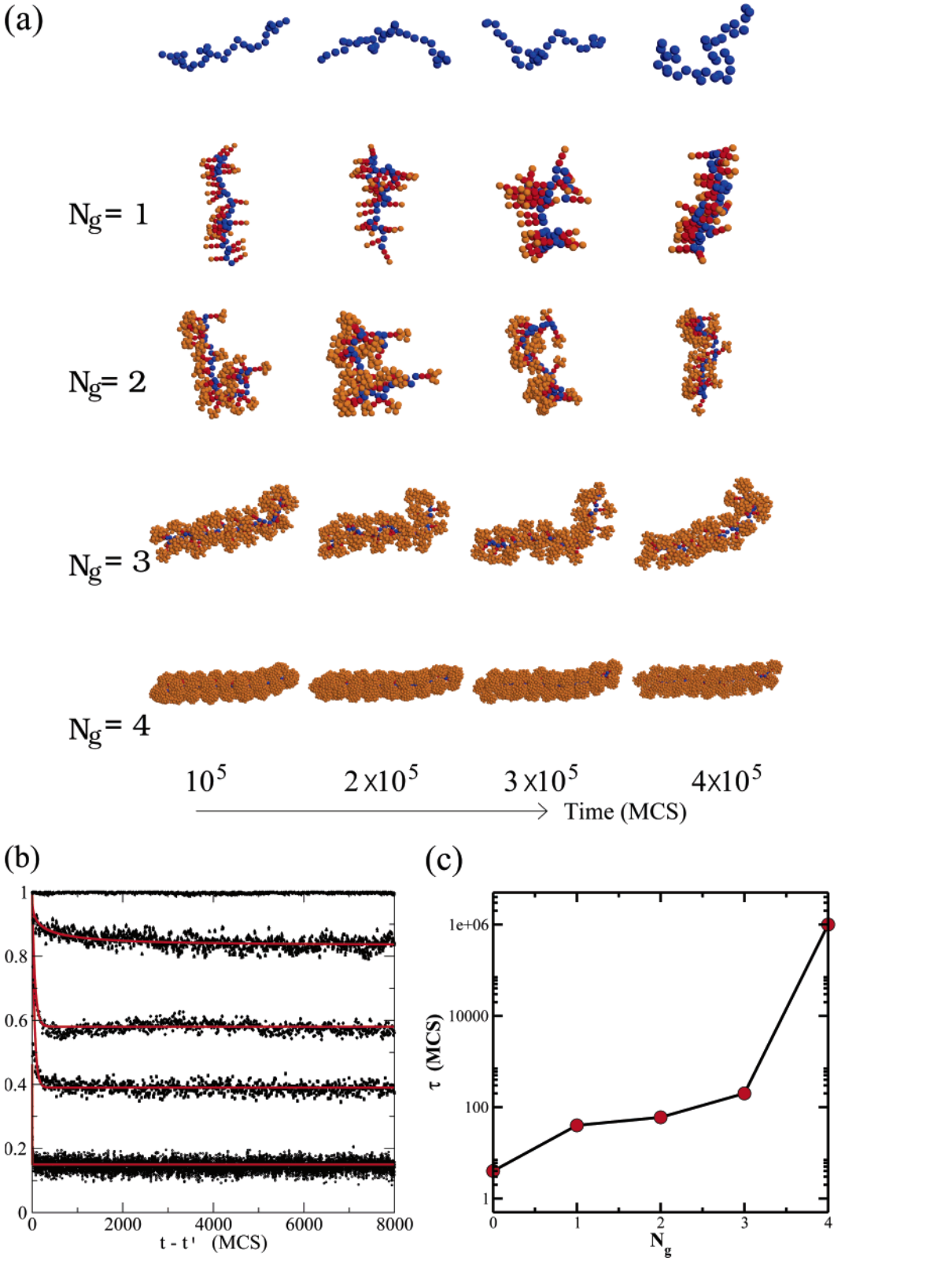

Figure 5. (a) Snapshots of configurations from the simulations for different number of generations characterizing dendron units; the backbone, connector, and dendron units are shown by blue, red, and gold spheres, respectively. The configurations change quickly for low values of N_g ($N_g < 3$) and extremely slowly for higher values ($N_g \geq 3$). (b) Autocorrelation function $A(t, t')$ vs $(t - t')$ for $N_g = 0-4$. The solid red lines show the respective fits with a functional form $A \exp(-[(t - t')/\tau]^{\beta}) + b$ where β is the stretching exponent. b accounts for the long-time saturation of the function and depends on N_g because it depends on chain conformational statistics. For $N_g \geq 3$, β is smaller than unity (Debye value). (c) Variation of the relaxation time τ, calculated from the fits described above, with N_g. The generation number behaves as an inverse temperature. It shows a singularity (within simulation time) at $N_g = 4$.

determine the dynamics of the backbone monomers. These effective constraints emerge naturally, but it is difficult to write down a simple facilitation rule corresponding to it at the present time. In facilitated Ising spin models, the postulated constraints become important upon cooling. For a dendronized polymer, the relative importance of constraints can be tuned by changing

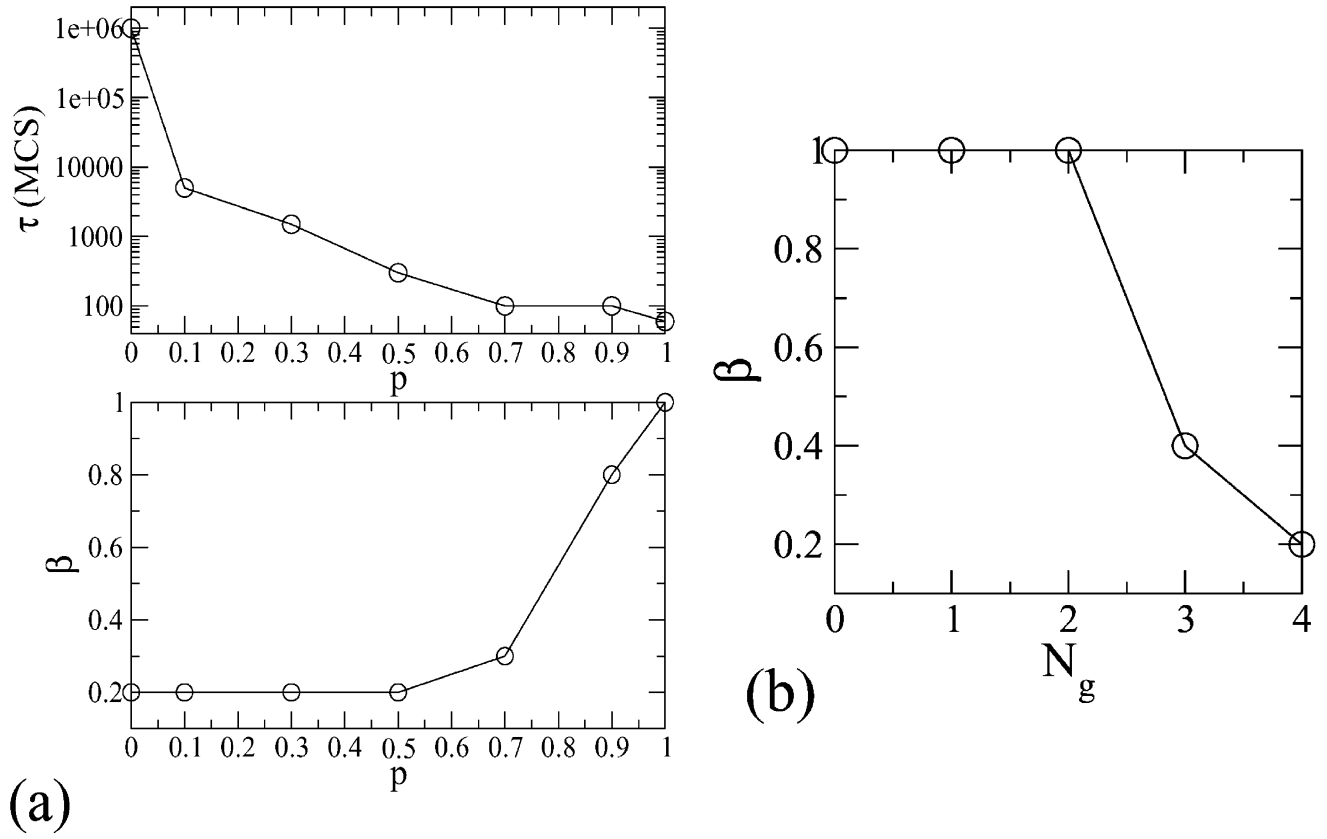

Figure 6. (a) Variation of the relaxation time τ (top) and stretching exponent (β) (bottom) with defect density (p) for $N_g = 4$. (b) Variation of β with N_g with no defects.

molecular architecture. For example, N_g can be viewed to be analogous to inverse temperature. Facilitated Ising spin models are characterized by dynamic slowing down that is not caused by an underlying thermodynamic singularity. It has been impossible to carry out experimental studies of such purely dynamic phase transitions in trajectory space by cooling bulk substances. This is because it is difficult to prove that a bulk liquid does not have a thermodynamic singularity at low temperatures that cannot be accessed by experiments. For dendronized polymers, our experiments and computer simulations (Figure 3) suggest that there exist no thermodynamic singularities over a range of values of N_g and p that do, however, exhibit signatures of dynamic slowing down as N_g increases. Thus, we believe that dendronized polymers provide an example (to our knowledge, the first one) of an experimental system that can be used to study the physics of phase transitions in space−time predicted by facilitated Ising models.

However, some difficult issues pertinent to the study of glass-forming liquids could emerge here as well. For dendronized polymers with a large value of N_g (≥ 4), our simulations show that the segment density near the periphery can be close to 0.56. This density is above the value ($\varphi_c = 0.494$) required for a system of monodisperse hard spheres to undergo a liquid-to-solid transition.[13] Therefore, the segments probably are in a "jammed" state near the periphery of the dendronized chain, and because of the constraints imposed by the dendrons on the backbone, the dynamics of the backbone monomers is also affected. However, whether the transition from a liquid phase to a solid phase in a system of hard spheres as the volume fraction increases is a thermodynamic glass transition remains an open question.[13,36] Though early simulations[12] and experiments[11,37] on colloidal systems suggest a thermodynamic glass transition, a recent MD simulation by Rintoul and Torquato[13,36] shows that the system of monodisperse hard spheres crystallizes for all volume fraction above φ_c. However, the dendrons are not monodisperse hard spheres, so for $N_g \geq 4$, the possibility of a thermodynamic transition cannot be ruled out. At the same time, in our system, for $N_g = 3$, the segment density is far below $\varphi_c = 0.494$. Thus, the glassy behavior of the system as reflected by the stretched exponential decay of the autocorrelation function appears to be due to dynamic facilitation. Future theoretical and experimental study of the single-molecule physics of dendronized chains will illuminate some of these issues further.

The results shown in Figures 5 and 6 show that our results resemble those described before for facilitated Ising spin models. As a consequence of constrained dynamics in facilitated Ising spin models, a "jammed" region can become mobile only if the adjacent regions are "unjammed". It is intuitively apparent that for a dendronized polymer with sufficiently large dendrons this physical situation is realized. Thus, as in facilitated Ising spin models, we expect the existence of dynamic heterogeneities in space−time.[8,35,38] The dynamic correlations of the quantity $\sigma(i)$ allow us to monitor the existence of such spatially heterogeneous dynamics. Figure 7 shows that as the number of generations increases dynamic trajectories of $\sigma(i)$ exhibit a structure that resembles the properties of a class of facilitated Ising spin models upon cooling. We also found that a set of order parameters less restrictive than $\sigma(i)$ also exhibit signatures of spatially heterogeneous dynamics, which suggests existence of a continuous scalar order parameter in the system.

Our results and arguments suggest that the dynamics characterizing conformational fluctuations of a dendronized polymer may map onto constrained dynamic models such as facilitated Ising spin models. Furthermore, for large values of N_g, the possibility of underlying thermodynamic transitions is worth

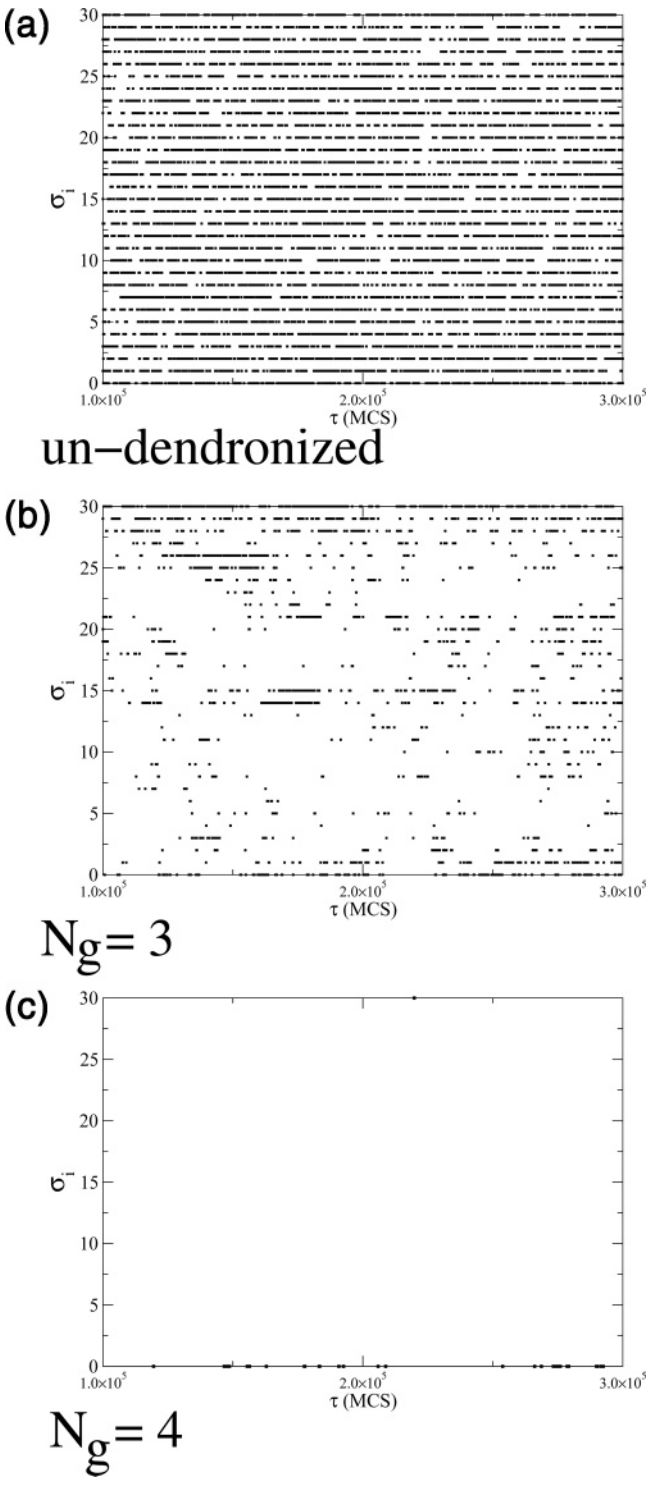

Figure 7. Trajectories of $\sigma(i)$ shown for the backbone (a) with no dendrons and with dendrons characterized by (b) $N_g = 3$ and (c) $N_g = 4$. The points where $\sigma(i) = 1$ are shown in black. Compare the uniformly distributed black and white regions in a with correlated regions in b and c.

exploring. Thus, single-molecule experiments where conformational fluctuations of a single dendronized polymer are studied may provide deep insights into factors underlying glassy dynamics. In particular, we suggest measurements of the quantity C using fluorescently labeled dendronized polymers that differ only in the number of generations that constitutes a dendron. Such measurements may be possible using single-molecule experiments[39,40] in the presence of quenchers.[39] Dynamic light scattering experiments[41] on dilute solutions of dendronized polymers may also enable us to probe the conformational dynamics of dendronized polymer chains. Dynamical heterogeneities in glass formers manifest in intermittency in the dynamics,[42−44] which triggers the violation of fluctuation−dissipation relations. The experiments mentioned above can also probe such behavior.

Conclusions

Dendronized polymers offer a new genre of molecules that can have rich and complex equilibrium and dynamic behavior with significant applications in nanotechnology. Here we have described changes in the thermodynamic and dynamic features of a single dendronized polymer as the number of generations characterizing each dendron increases. Our experiments and computer simulations show that there is a smooth crossover from a completely flexible chain to a rigid rodlike structure as the number of generations increases. Our computer simulations show that the dynamics of backbone configuration fluctuations exhibits glassy dynamics as the number of generations increases. Thus, a dendronized polymer is a single molecule that can serve as an experimental platform where the physics (thermodynamics and dynamics) of glassy systems can be studied by tuning molecular architecture. This single-molecule glassy system that we have described also constitutes a building block for creating self-assembled nanoscale objects for advanced applications.

Acknowledgment. This paper is dedicated to celebrating Professor David Chandler's 60th birthday. We thank D. Chandler, S. Chempath, N. Lacevic, M. Hagan, and J. Liu for discussions. We also thank two reviewers for very insightful remarks. We gratefully acknowledge the financial support provided by the Department of Energy (Materials Sciences Division, Lawrence Berkeley National Laboratory). This work was supported by the Department of Energy, contract no. DE-AC03-76SF00515. M.Y. thanks the Japan Society for the Promotion of Science (JSPS) for the Japan Overseas Fellowship for Young Scientists.

References and Notes

(1) Tomalia, D. A.; Baker, H.; Dewald, J.; Hall, M.; Kallos, G.; Martin, S.; Roeck, J.; Ryder, J.; Smith, P. *Polym. J.* **1985**, *17*, 117.
(2) Schluter, A. D.; Rabe, J. P. *Angew. Chem., Int. Ed.* **2000**, *39*, 864.
(3) Fréchet, J. M. J. *Proc. Natl. Acad. Sci. U.S.A.* **2002**, *99*, 4782.
(4) Gennes, P. G. d. *Scaling Concepts in Polymer Physics*; Cornell University Press: Ithaca, NY, 1979, p 25.
(5) Garrahan, J. P.; Chandler, D. *Phys. Rev. Lett.* **2002**, *89*, 035704.
(6) Fredrickson, G. H.; Andersen, H. C. *Phys. Rev. Lett.* **1984**, *53*, 1244.
(7) R. G. Palmer, D. L. S., E. Abrahams, P. W. Anderson. *Phys. Rev. Lett.* **1984**, *53*, 958.
(8) Garrahan, J. P.; Chandler, D. *Proc. Natl. Acad. Sci. U.S.A.* **2003**, *100*, 9710.
(9) Ritort, F.; Sollich, P. *Adv. Phys.* **2003**, *52*, 219.
(10) Ecker, C.; Severin, N.; Shu, L. J.; Schluter, A. D.; Rabe, J. P. *Macromolecules* **2004**, *37*, 2484.
(11) Pusey, P. N.; Vanmegen, W. *Nature* **1986**, *320*, 340.
(12) Speedy, R. J. *J. Chem. Phys.* **1994**, *100*, 6684.
(13) Rintoul, M. D.; Torquato, S. *Phys. Rev. Lett.* **1996**, *77*, 4198.
(14) Williams, S. R.; Snook, I. K.; van Megen, W. *Phys. Rev. E* **2001**, *6402*.
(15) Gotze, W.; Sjogren, L. *Rep. Prog. Phys.* **1992**, *55*, 241.
(16) Stillinger, F. H. *Science* **1995**, *267*, 1935.
(17) Sastry, S.; Debenedetti, P. G.; Stillinger, F. H. *Nature* **1998**, *393*, 554.
(18) Sillescu, H. *J. Non-Cryst. Solids* **1999**, *243*, 81.
(19) Xia, X. Y.; Wolynes, P. G. *Proc. Natl. Acad. Sci. U.S.A.* **2000**, *97*, 2990.
(20) Grayson, S. M.; Fréchet, J. M. J. *Macromolecules* **2001**, *34*, 6542.
(21) *Monte Carlo and Molecular Dynamics Simulations in Polymer Science*; Binder, K., Ed.; Oxford University Press: Oxford, U.K., 1995.

(22) Gerroff, I.; Milchev, A.; Binder, K.; Paul, W. *J. Chem. Phys.* **1993**, *98*, 6526.
(23) Mayo, S. L.; Olafson, B. D.; Goddard, W. A. *J. Phys. Chem.* **1990**, *94*, 8897.
(24) Metropolis, N.; Rosenbluth, A. W.; Rosenbluth, M. N.; Teller, A. H.; Teller, E. *J. Chem. Phys.* **1953**, *21*, 1087.
(25) Yoshida, M.; Fresco, Z. M.; Ohnishi, S.; Fréchet, J. M. J. *Macromolecules* **2005**, *38*, 334.
(26) Yamakawa, H. *Helical Wormlike Chains in Polymer Solutions*; Springer-Verlag: Berlin, 1997.
(27) Welch, P.; Muthukumar, M. *Macromolecules* **1998**, *31*, 5892.
(28) Zimm, B. H.; Stockmayer, W. H. *J. Chem. Phys.* **1949**, *17*, 1301.
(29) It could be argued that for larger values of N_g the simulation results do not correspond to equilibrium averages. As we show in Figure 5c, the simulations do correspond to equilibrium averages. For $N_g = 3$, dynamic anomalies are already manifested. Thus, the value of conditions that do not correspond to thermodynamic anomalies does result in glassy dynamics.
(30) Stauffer, D.; Aharony, A. *Introduction to Percolation Theory*, 2nd ed.; Taylor & Francis: London, 1992.
(31) Pike, G. E.; Seager, C. H. *Phys. Rev. B* **1974**, *10*, 1421.
(32) Gawlinski, E. T.; Stanley, H. E. *J. Phys. A: Math. Gen.* **1981**, *14*, L291.
(33) Kob, W.; Andersen, H. C. *Phys. Rev. Lett.* **1994**, *73*, 1376.
(34) Kob, W.; Andersen, H. C. *Phys. Rev. E* **1995**, *51*, 4626.
(35) Weeks, E. R.; Crocker, J. C.; Levitt, A. C.; Schofield, A.; Weitz, D. A. *Science* **2000**, *287*, 627.
(36) Rintoul, M. D.; Torquato, S. J. *Chem. Phys.* **1996**, *105*, 9258.
(37) Vanblaaderen, A.; Wiltzius, P. *Science* **1995**, *270*, 1177.
(38) Kob, W.; Donati, C.; Plimpton, S. J.; Poole, P. H.; Glotzer, S. C. *Phys. Rev. Lett.* **1997**, *79*, 2827.
(39) Yang, H.; Xie, S. X. *J. Chem. Phys.* **2002**, *117*, 10965.
(40) Xie, X. S.; Dunn, R. C. *Science* **1994**, *265*, 361.
(41) Goinga, H. T.; Pecora, R. *Macromolecules* **1991**, *24*, 6128.
(42) Cipelletti, L.; Bissig, H.; Trappe, V.; Ballesta, P.; Mazoyer, S. *J. Phys.: Condens. Matter* **2003**, *15*, S257.
(43) Buisson, L.; Bellon, L.; Ciliberto, S. *J. Phys.: Condens. Matter* **2003**, *15*, S1163.
(44) Merolle, M.; Garrahan, J. P.; Chandler, D. *cond-mat/0501180* 2005.